

Topology Optimization of Structures under Constraints on First Passage Probability

Junho Chun

Doctoral Student, Dept. of Civil and Environmental Engineering, Univ. of Illinois, Urbana-Champaign, USA

Junho Song

Associate Professor, Dept. of Civil and Environmental Engineering, Seoul National Univ., Seoul, Korea

Glaucio H. Paulino

Raymond Jones Chair, School of Civil and Environmental Engineering, Georgia Institute of Technology, Atlanta, USA

ABSTRACT: A new method is proposed to incorporate the first passage probability into stochastic topology optimization using sequential compounding method (Kang and Song 2010). Parameter sensitivities of the first passage probability in the probabilistic constraint are derived to facilitate the use of gradient-based optimizer for efficient topology optimization. The proposed method is applied to building structures subjected to stochastic ground motion to find optimal bracing systems which can resist future realization of stochastic excitations while achieving a desired level of reliability.

Optimal design of a lateral load-resisting system of a structure is one of the essential tasks in structural engineering as it is directly linked to building safety and operation. In particular, reliable operation and safety under stochastic excitations by natural hazards such as earthquake, wind loads are major design objectives. However, deterministic description of future realization of a random process is frequently limited because only a set of few time histories are available. Therefore, a probabilistic prediction of structural responses based on random vibration analysis is much needed in the process for optimal design. To address this issue, the authors performed a study of topology optimization of structures under stochastic excitations (Chun et al. in review). In the study, random vibration analysis by a discrete representation method (Der Kiureghian 2000) and structural reliability theory were integrated into topology optimization framework. In addition, the authors developed the system reliability-based topology optimization framework under stochastic excitations (Chun et al. 2013) to consider system failure events with statistical dependency using the matrix-based system reliability method (Song and Kang 2009). The

developed method helps satisfy probabilistic constraints on a system failure event, which consists of multiple limit-states defined in terms of different locations, failure modes and time points as it optimizes a structural system. Chun et al. (in review) has evaluated an instantaneous failure probability of the structure subjected to random excitations at a discrete time point. However, a more practical application in engineering can be achieved if the failure probability is evaluated for exceedance event over a time interval. This helps promote the use of the proposed stochastic topology optimization framework for the design of lateral load-resisting system under stochastic excitations. Thus, in this paper, a stochastic topology optimization framework is proposed to handle probabilistic constraints on the first passage probability.

1. RANDOM VIBRATION ANALYSIS USING DISCRETE REPRESENTATION METHOD

1.1. Discrete representation of stochastic process

The discrete representation method (Der Kiureghian 2000) discretizes a continuous

stochastic process with a finite number of standard normal random variables. For example, a zero-mean Gaussian process $f(t)$ can be discretized as:

$$f(t) = \sum_{i=1}^n v_i s_i(t) = \mathbf{s}(t)^T \mathbf{v} \quad (1)$$

where $\mathbf{s}(t)$ denotes a vector of deterministic basis functions, which is determined from the spectral characteristics of the process (Der Kiureghian 2000), and \mathbf{v} is a vector of n uncorrelated standard normal random variables.

1.2. Characterization of linear system under stochastic excitations

The displacement time history $u(t)$ of a linear system subjected to stochastic excitations, can be determined by using Duhamel's integral and Eq. (1), i.e.

$$\begin{aligned} u(t) &= \int_0^t f(\tau) h_s(t-\tau) d\tau = \int_0^t \sum_{i=1}^n v_i s_i(\tau) h_s(t-\tau) d\tau \\ &= \sum_{i=1}^n v_i a_i(t) = \mathbf{a}(t)^T \mathbf{v}, \quad a_i(t) = \int_0^t s_i(\tau) h_s(t-\tau) d\tau \end{aligned} \quad (2)$$

where $h_s(t)$ is the unit impulse response function of the degree-of-freedom of interest, and $\mathbf{a}(t)$ denotes a vector of deterministic basis functions. Then, failure events defined in terms of responses can be described in the space of standard normal random variable \mathbf{v} (Der Kiureghian 2000).

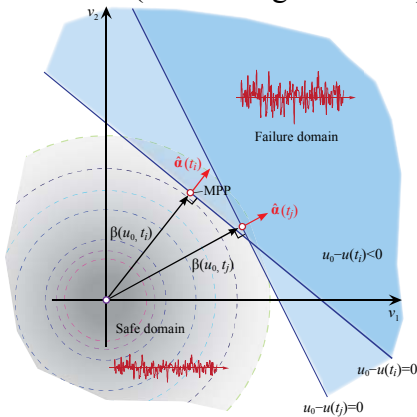


Figure 1 : Geometric representation of instantaneous failure at time t_i and t_j in standard normal space.

For example, the 'instantaneous' failure event, i.e. the event of a response at a certain time $t = t_i$

exceeding a prescribed threshold u_0 , is represented by the linear half space $u_0 - u(t_i) = u_0 - \mathbf{a}(t_i)^T \mathbf{v} \leq 0$ as shown in Figure 1. From the geometric interpretation, a reliability index can be computed as a closed-form solution, i.e.

$$\beta(u_0, t_i) = u_0 / \|\mathbf{a}(t_i)\| = \hat{\mathbf{a}}(t_i)^T \mathbf{v}^* \quad (3)$$

where $\hat{\mathbf{a}}$ denotes the negative normalized gradient vector of the limit-state function evaluated at the most probable failure point \mathbf{v}^* .

2. FIRST-PASSAGE PROBABILITY

The first passage probability is commonly utilized to find the probability of the failure event described within a time interval (VanMarcke 1975, Song and Der Kiureghian 2006, Fujimura and Der Kiureghian 2007). One of the available approaches for formulating the first passage probability is defining the problem as a series system problem such as:

$$P(E_{\text{sys}}) = P(x < \max_{0 < t < t_n} |u(t)|) = P\left(\bigcup_{i=1}^n |u(t_i)| > u_0\right) \quad (4)$$

The first passage probability then requires evaluation of component events at each time point within an interval. Moreover, an efficient, reliable and robust algorithm is required to evaluate system failure probability with statistical dependency between the component events fully considered. To address these requirements, the sequential compounding method (SCM; Kang and Song 2010) is adopted in this study.

3. SEQUENTIAL COMPOUNDING METHOD

The sequential compounding method is a system reliability method that compounds component events coupled by union or intersection sequentially until a single compound event represents the system event. Whenever two components are compounded, the probability of the new compound event is obtained while the correlation coefficients between the new compound event and each of the other remaining component events are computed. For instance, compounding two component events in a series system can be described as

$$P(E_1 \cup E_2 \cup \dots \cup E_n) = P(E_{1 \text{ or } 2} \cup E_3 \cup \dots \cup E_n) \quad (5)$$

The reliability index $\beta_{1\text{or}2}$ of the compound event $E_{1\text{or}2}$ can be determined as follow:

$$\beta_{1\text{or}2} = -\Phi^{-1}[1 - P(\bar{E}_1 \cap \bar{E}_2)] = \Phi^{-1}[\Phi_2(\beta_1, \beta_2; \rho_{1,2})] \quad (6)$$

where Φ and Φ_2 respectively denote the marginal and bi-variate cumulative distribution function (CDF) of standard normal random variable(s).

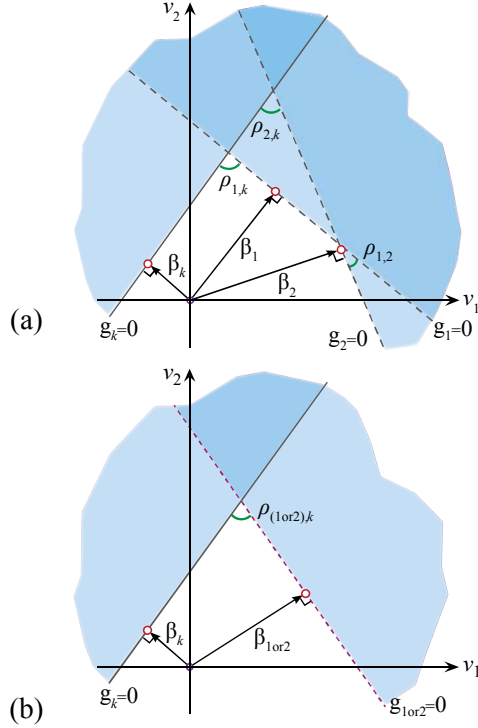


Figure 2: SCM procedure. (a) system probability of three events; (b) compound event of E_1 and E_2 and an updated correlation coefficient.

The correlation coefficients between the compound event and the remaining events, i.e. $\rho_{(1\text{or}2),k}$, $k = 3, \dots, n$ are determined such that

$$\int_{\Omega_u} \varphi(z_1, z_2, z_3; \rho_{1,2}, \rho_{1,k}, \rho_{2,k}) dz = \Phi_2(-\beta_{1\text{or}2}, -\beta_k; \rho_{(1\text{or}2),k}) \quad (7)$$

where \mathbf{z} denotes a vector of standard normal random variables, φ is the joint probability density function of \mathbf{z} , and Ω_u represents the domain of the system event as

$$\Omega_u = [(Z_1 \leq -\beta_1) \cup (Z_1 \leq -\beta_2)] \cap (Z_k \leq -\beta_k) \quad (8)$$

$\rho_{(1\text{or}2),k}$ in Eq. (7) is obtained numerically by using nonlinear programming. The sequential compounding procedure of three events is

illustrated in Figure 2. More details on an efficient scheme to find $\rho_{(1\text{or}2),k}$ and compounding two components coupled by intersection can be found in Kang and Song (2010). The SCM is implemented to compute the first-passage probability in the proposed method because the SCM can provide the probability and parameter sensitivities of a system consisting of a large number of components.

4. PARAMETETRIC SENSITIVITY OF SYSTEM RELIABILITY USING SCM

Reliability based design/topology optimization (RBDO/RBTO) can be efficiently performed if parameter sensitivities of the probability can be readily computed. In this paper, the first passage probability is considered as a probabilistic constraint in topology optimization. Therefore, sensitivity analysis of system reliability consisting of many component events is required. Integrating SCM with the proposed method leads to significant reduction of computational cost for the reliability analysis in the developed topology optimization framework.

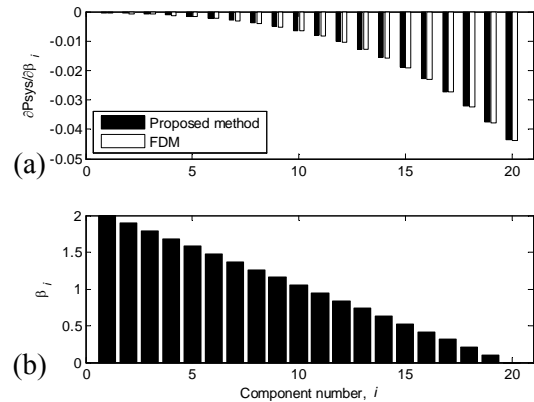


Figure 3: Sensitivities of series system with 20 components (unequal reliability indices and equal correlation coefficients, 0.5): (a) sensitivity comparison between the proposed method and finite difference method, and (b) component reliability indices consisting of the series system.

To this end, the authors further developed the SCM to compute parameter sensitivities efficiently (Chun et al. 2015). Figure 3(a) shows numerical results of the sensitivity analysis for a series system with 20 components.

5. TOPOLOGY OPTIMIZATION UNDER FIRST PASSAGE PROBABILITY

Topology optimization (Bendsøe and Sigmund 2003) aims to find the optimal material distributions in a design domain Ω subjected to tractions and displacement boundary conditions while satisfying given design constraints. In this paper, we consider a linear elastic and isotropic constituent material with an elasticity tensor \mathbf{D}_0 . Solid Isotropic Material with Penalization (SIMP; Bendsøe and Sigmund 1999) model is adopted in which a smooth convex function $\psi: R \rightarrow [0, 1]$ is defined by a power function representation, i.e.

$$\psi(x) = x^p \quad (9)$$

where $p > 0$ is a penalization factor and x is a filtered density $\tilde{\rho}_e(\mathbf{d})$ with a vector of deterministic design variables, \mathbf{d} . The SIMP model expresses an elasticity tensor of an isotropic material in the state of plane stress as:

$$\mathbf{D}(\tilde{\rho}_e(\mathbf{d})) = \frac{\psi(\tilde{\rho}_e(\mathbf{d})) \cdot E_0}{1 - \nu^2} \cdot \begin{bmatrix} 1 & \nu & 0 \\ \nu & 1 & 0 \\ 0 & 0 & (1 - \nu)/2 \end{bmatrix} \quad (10)$$

where ν is the Poisson's ratio, and E_0 is the elasticity tensor of the solid material, where the density is 1. The filtered element density can be obtained by using a density filtering method such as the projection technique (e.g. Guest et al. 2004, Sigmund 2007) to avoid checkerboard-patterns and to achieve a minimum length scale. By using a linear "hat" kernel of radius r , the element density can be computed as a weighted average of the design variables within an influence domain Ω_e such as:

$$\tilde{\rho}_e(\mathbf{d}) = \sum_{j \in \Omega_e} w_j d_j / \sum_{j \in \Omega_e} w_j \quad (11)$$

Where $w_j = (r - r_j)/r > 0$ is a weight, and r_j is the distance between the centroids of element e and element j , which lies within the radius r of element e . In order to avoid singularity of a stiffness matrix in finite element analysis, one needs to set a lower bound on the element density $\tilde{\rho}_e(\mathbf{d})$ i.e., $0 < \tilde{\rho}_{\min} \ll \tilde{\rho}_e(\mathbf{d}) \leq 1$. Using the SIMP model, the stiffness matrix of the e^{th} element and its

sensitivity are obtained as follows in the element-based computational framework (Bendsøe and Sigmund 2003):

$$\mathbf{K}_e(\tilde{\rho}_e) = \tilde{\rho}_e^p \mathbf{K}_e^0, \quad \partial \mathbf{K}_e(\tilde{\rho}_e) / \partial \tilde{\rho}_e = p \tilde{\rho}_e^{p-1} \mathbf{K}_e^0 \quad (12)$$

A formulation of topology optimization under stochastic excitation with the first passage probability constraint can be formulated as follows:

$$\begin{aligned} \min_{\mathbf{d}} \quad & f(\tilde{\rho}) \\ \text{s.t.} \quad & P\left(\bigcup_{i=1}^n (g_i : u(t_i) > u_0)\right) = P(E_{\text{sys}} : \beta_1, \dots, \beta_n) \leq P_{\text{sys}}^t \\ & 0 < \varepsilon \leq \tilde{\rho}(\mathbf{d}) \leq 1 \quad \forall \mathbf{d} \in \Omega \\ & \text{with } \mathbf{M}(\tilde{\rho})\ddot{\mathbf{u}}(t, \tilde{\rho}) + \mathbf{C}(\tilde{\rho})\dot{\mathbf{u}}(t, \tilde{\rho}) + \mathbf{K}(\tilde{\rho})\mathbf{u}(t, \tilde{\rho}) = \mathbf{f}(t, \tilde{\rho}) \end{aligned} \quad (13)$$

where n denotes the total number of time points during stochastic excitations, \mathbf{M} , \mathbf{C} and \mathbf{K} are the mass, damping and stiffness matrices of the design domain, respectively, and $\ddot{\mathbf{u}}$, $\dot{\mathbf{u}}$, \mathbf{u} and \mathbf{f} are the acceleration, velocity, displacement and external force vectors at time t , respectively. We omitted the dependence of filtered densities $\tilde{\rho}$ on the design variables \mathbf{d} , $\tilde{\rho} = \tilde{\rho}(\mathbf{d})$.

6. SENSITIVITY ANALYSIS: FIRST PASSAGE PROBABILITY

Sensitivity analysis is an essential procedure in order to use gradient-based optimization algorithms. A method of adjoint sensitivity analysis for probabilistic constraints is derived as follows.

6.1. Adjoint sensitivity analysis

Sensitivity of the probabilistic constraint on the first passage probability is computed from the following expression.

$$\begin{aligned} & \frac{\partial P(E_{\text{sys}} : \beta_1(\tilde{\rho}), \dots, \beta_n(\tilde{\rho}))}{\partial d_i} \\ &= \sum_{j=1}^n \left(\frac{\partial P(E_{\text{sys}} : \beta_1(\tilde{\rho}), \dots, \beta_n(\tilde{\rho}))}{\partial \beta_j} \cdot \sum_{i=1}^{n_e} \frac{\partial \beta_j(\tilde{\rho})}{\partial \tilde{\rho}_i} \cdot \frac{\partial \tilde{\rho}_i}{\partial d_i} \right) \quad (14) \\ &= \mathbf{P}^T \sum_{j=1}^n \left(c_j \cdot \frac{\partial \beta_j(\tilde{\rho})}{\partial \tilde{\rho}_i} \right) \end{aligned}$$

where \mathbf{P}^T denotes a filtering matrix computed from Eq. (11). $c_j = \partial P(E_{sys}) / \partial \beta_j$ can be obtained as in Chun et al. (2015). The partial derivative $\partial \beta_j / \partial \tilde{\rho}_i$ is obtained from the following expression.

$$\frac{\partial \beta_j}{\partial \tilde{\rho}_i} = - \frac{u_0 \cdot \left(\sum_{k=1}^j a_k(t_j, \tilde{\rho}) \cdot \frac{\partial a_k(t_j, \tilde{\rho})}{\partial \tilde{\rho}_i} \right)}{\left(\sum_{k=1}^j a_k(t_j, \tilde{\rho})^2 \right)^{1.5}} \quad (15)$$

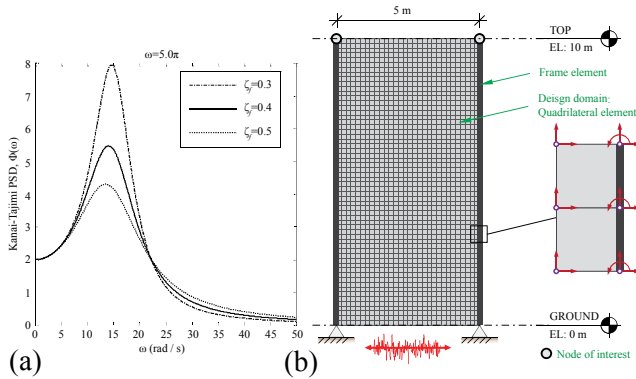


Figure 4: (a) Kanai-Tajimi power spectral density (PSD); (b) Design domain and loading configuration.

When a uniform time step size is used, i.e. $t_i - t_{i-1} = \Delta t$, $i = 1, 2, \dots, n$ and $t_n = t_0$, Eq. (14) can be rewritten as follows:

$$\begin{aligned} \frac{\partial P(E_{sys})}{\partial d_i} &= \mathbf{P}^T \left[(\chi_1 + \chi_2 + \dots + \chi_n) a_n(t_n, \tilde{\rho}) \frac{\partial a_n(t_n, \tilde{\rho})}{\partial \tilde{\rho}_i} \right. \\ &\quad \left. + \dots + \chi_n(t_n, \tilde{\rho}) a_1(t_n, \tilde{\rho}) \frac{\partial a_1(t_n, \tilde{\rho})}{\partial \tilde{\rho}_i} \right] \\ &= \mathbf{P}^T \left(\sum_{l=m}^n \chi_l a_{n-l+1}(t_n, \tilde{\rho}) \frac{\partial a_{n-l+1}(t_n, \tilde{\rho})}{\partial \tilde{\rho}_i} \right), \quad m = 1, \dots, n \end{aligned} \quad (16)$$

where

$$\chi_l = -c_l u_0 / \left(\sum_{k=1}^l a_k(t_l, \tilde{\rho})^2 \right)^{3/2} \quad (17)$$

Pre-multiplying the discretized adjoint system from the governing system equation in Eq. (13) with a n_{dof} dimensional adjoint variable vector λ_{n-j+1} and adding to right-hand side terms of Eq. (16), the following expression is obtained:

$$\begin{aligned} \frac{\partial P(E_{sys})}{\partial d_i} &= \mathbf{P}^T \left(\sum_{l=m}^n \chi_l a_{n-l+1}(t_n, \tilde{\rho}) \frac{\partial a_{n-l+1}(t_n, \tilde{\rho})}{\partial \tilde{\rho}_i} \right) \\ &\quad + \sum_{j=1}^n \lambda_{n-j+1}^T \left[\frac{\partial \underline{\mathbf{A}}(\tilde{\rho})}{\partial \tilde{\rho}_j} \cdot \mathbf{u}(t_j, \tilde{\rho}) + \underline{\mathbf{A}}(\tilde{\rho}) \cdot \frac{\partial \mathbf{u}(t_j, \tilde{\rho})}{\partial \tilde{\rho}_j} \right. \\ &\quad \left. - (0.5 + \gamma - 2\eta)(\Delta t)^2 \frac{\partial \mathbf{f}(t_{j-1}, \tilde{\rho})}{\partial \tilde{\rho}_j} \right. \\ &\quad \left. - \eta(\Delta t)^2 \frac{\partial \mathbf{f}(t_j, \tilde{\rho})}{\partial \tilde{\rho}_j} - (0.5 - \gamma + \eta)(\Delta t)^2 \frac{\partial \mathbf{f}(t_{j-2}, \tilde{\rho})}{\partial \tilde{\rho}_j} \right. \\ &\quad \left. + \frac{\partial \underline{\mathbf{B}}(\tilde{\rho})}{\partial \tilde{\rho}_j} \cdot \mathbf{u}(t_{j-1}, \tilde{\rho}) + \underline{\mathbf{B}}(\tilde{\rho}) \cdot \frac{\partial \mathbf{u}(t_{j-1}, \tilde{\rho})}{\partial \tilde{\rho}_j} \right. \\ &\quad \left. + \frac{\partial \underline{\mathbf{E}}(\tilde{\rho})}{\partial \tilde{\rho}_j} \cdot \mathbf{u}(t_{j-2}, \tilde{\rho}) + \underline{\mathbf{E}}(\tilde{\rho}) \cdot \frac{\partial \mathbf{u}(t_{j-2}, \tilde{\rho})}{\partial \tilde{\rho}_j} \right] \end{aligned} \quad (18)$$

More details of the adjoint sensitivity analysis can be found in Chun et al. (in review).

7. NUMERICAL APPLICATIONS

7.1. Comparison of the finite difference method and the adjoint method

The derived adjoint sensitivity method was compared with the finite difference method (FDM) to verify accuracy and efficiency. For comparison, The stochastic seismic excitation $f(t)$ is modeled as a filtered white-noise process using the Kanai-Tajimi filter model with the intensity Φ_0 (Figure 4(a)). The force vector in Eq. (13) is replaced with an inertial force vector of $\mathbf{f} = -\mathbf{M}(\rho)\mathbf{l}f(t)$ where the vector \mathbf{l} represents directional distribution of masses with unity. The structural columns represented by two vertical lines as shown in Figure 4(b) are modeled by frame elements whose densities remain unchanged throughout the optimization process. Young's modulus $E = 21,000$ MPa and mass density $\rho = 2,400$ kg/m³ are used as material properties for both the quadrilateral and frame elements. The damping matrix is constructed using a Rayleigh damping model. Table 1 summarizes the Kanai-Tajimi filter parameters of dominant frequency ω_f and bandwidth ζ_f , column size, time interval of interest, and the threshold value u_0 of the average drift ratio at each time point.

Table 1. Parameters used for sensitivity analysis: design domain, probabilistic constraint and ground motion model.

ω_f	ζ_f	Φ_0	Column size	t	u_0
			m	sec	
5π	0.4	450	0.4 x 0.4	4.0	0.02

At each time point, a component limit state is described as an event that the average inter-story drift ratio evaluated at nodes of interest in Figure 4(b) exceeds the given threshold values as:

$$E_f = u_0 - \left(\frac{(\mathbf{a}(t_0, \tilde{\boldsymbol{\rho}})_{Left}^T + \mathbf{a}(t_0, \tilde{\boldsymbol{\rho}})_{Right}^T) \mathbf{v}}{2 \cdot h} \right) \leq 0 \quad (19)$$

where h is the story height (10m). Figure 5 shows that sensitivities calculated by the finite difference method and the adjoint method match well. The computational cost of the adjoint sensitivity method is much less than the finite difference method as shown in Figure 6.

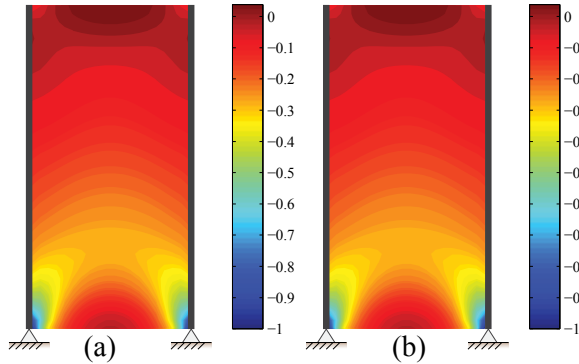


Figure 5: Normalized sensitivities by different approaches. (a) Finite difference method (FDM); (b) Adjoint method (AJM).

7.2. Example 1: Probabilistic constraint on first passage probability

The proposed topology optimization framework was applied to a multi-story building for identifying optimal bracing system under stochastic excitations. The design domain for topology optimization is shown in Figure 7(a). Kanai-Tajimi parameters in Section 7.1 are used except $\Phi_0=30$. The ground acceleration duration and a time step are 4.0s and 0.1s, respectively. A column size is $0.5m \times 0.5m$ and a threshold of inter-story drift ratio u_0 is 0.02. A filtering radius

r is 0.25m and a prescribed density 0.7 is applied uniformly throughout the mesh. The topology optimization problem can be formulated as:

$$\begin{aligned} & \min_{\tilde{\boldsymbol{\rho}}} \text{Volume}(\tilde{\boldsymbol{\rho}}) \\ & \text{s.t. } P\left(\bigcup_{i=1}^{40} (g_i : u(t_i) > u_0)\right) = P(E_{\text{sys}} : \beta_1, \dots, \beta_{40}) \leq P_{\text{sys}}^t \\ & \text{with } \mathbf{M}(\tilde{\boldsymbol{\rho}})\ddot{\mathbf{u}}(t, \tilde{\boldsymbol{\rho}}) + \mathbf{C}(\tilde{\boldsymbol{\rho}})\dot{\mathbf{u}}(t, \tilde{\boldsymbol{\rho}}) + \mathbf{K}(\tilde{\boldsymbol{\rho}})\mathbf{u}(t, \tilde{\boldsymbol{\rho}}) = \mathbf{f}(t, \tilde{\boldsymbol{\rho}}) \end{aligned} \quad (20)$$

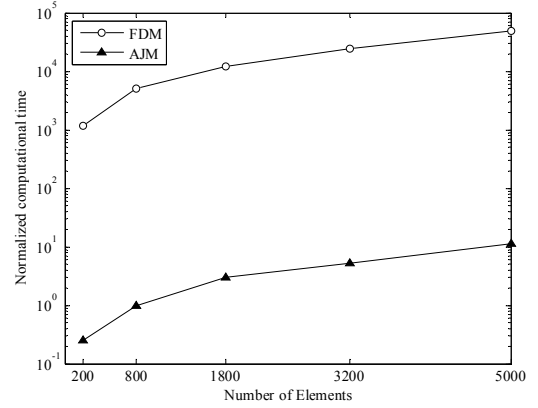


Figure 6: Normalized computational time.

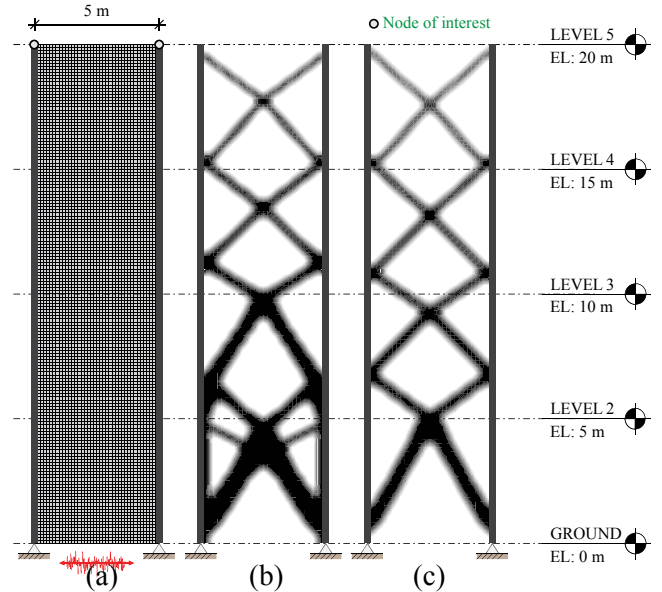


Figure 7: Topology optimization solutions to the multi-story building example. (a) design domain; (b) $\beta_{\text{sys}}^t = 3.0$, $P_{\text{sys}}^t = 0.13\%$; (c) $\beta_{\text{sys}}^t = 1.5$, $P_{\text{sys}}^t = 6.68\%$.

Topology optimization results corresponding to different target reliability indices are shown in Figure 7(b)-(c). As the target failure probability

decreases, the converged topologies become significantly different especially at the lower level. In particular, the intersection point of the bracing at the lower level moves up vertically and the thickness of the bracing increases at the lower level but remains relatively stable at higher levels. The convergence histories of the objective function and the system failure probability are shown in Figure 8.

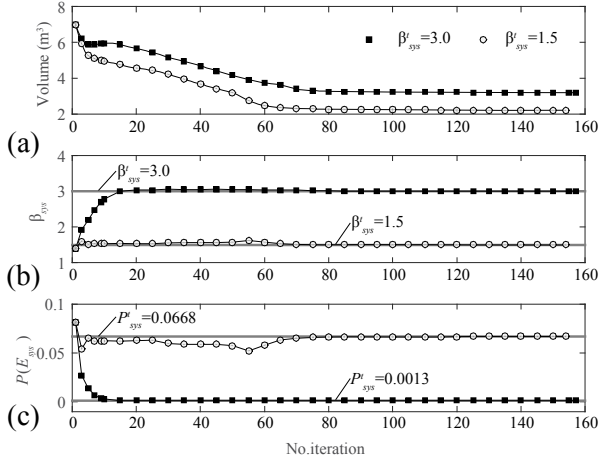


Figure 8: Convergence history. (a) volume; (b) reliability index; (c) failure probability.

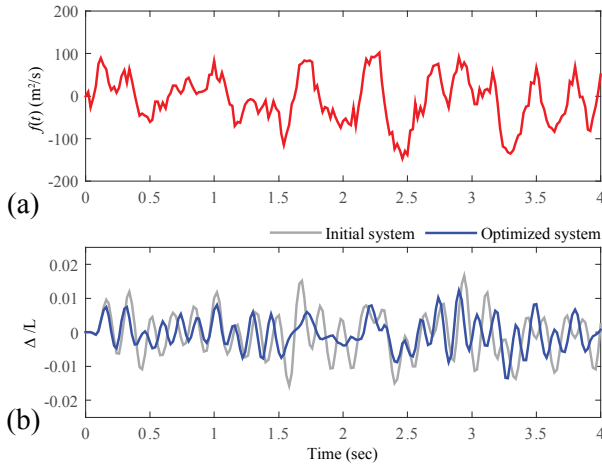


Figure 9: Dynamic response comparison of the problem shown in Fig. 7(b): (a) Input ground motion acceleration; (b) corresponding dynamic responses of the initial design and the optimal design.

Figure 9 shows time histories of inter-story drift ratios of the initial design and the optimal design for an input process randomly generated from the Kanai-Tajimi filter model. The optimized system shows improvement in dynamic

performance even though only 58% of the initial volume is used.

7.3. Example 2: Multiple probabilistic constraints on first passage probability

In this example, two probabilistic constraints given in terms of drift ratios are considered in Eq. (13) with the same modelling and optimization parameters in Section 7.2. The two limit-state functions of drift ratios are defined between the ground and the 2nd level; the 2nd and the 3rd level, respectively. Each limit state function is considered a component failure event. Thus, a topology optimization framework with two component probabilistic constraints is written as:

$$\begin{aligned} \min_{\mathbf{d}} \quad & \text{Volume}(\tilde{\mathbf{p}}) \\ \text{s.t.} \quad & P_1(E_{\text{sys}1} : \beta_{a,1}, \dots, \beta_{a,40}) \leq P'_{\text{sys}1} (= 0.0013) \\ & P_2(E_{\text{sys}2} : \beta_{b,1}, \dots, \beta_{b,40}) \leq P'_{\text{sys}2} (= 0.0013) \\ & \text{with } \mathbf{M}(\tilde{\mathbf{p}})\ddot{\mathbf{u}}(t, \tilde{\mathbf{p}}) + \mathbf{C}(\tilde{\mathbf{p}})\dot{\mathbf{u}}(t, \tilde{\mathbf{p}}) + \mathbf{K}(\tilde{\mathbf{p}})\mathbf{u}(t, \tilde{\mathbf{p}}) = \mathbf{f}(t, \tilde{\mathbf{p}}) \end{aligned} \quad (21)$$

In addition, system failure probability constraint combining those two constraints in Eq.(21) under statistical dependence can be considered in optimization as:

$$\begin{aligned} \min_{\mathbf{d}} \quad & \text{Volume}(\tilde{\mathbf{p}}) \\ \text{s.t.} \quad & P\left(\bigcup_{i=1}^{80} (g_i : u(t_i) > u_0)\right) \\ & = P(E_{\text{sys}} : \beta_{a,1}, \dots, \beta_{a,40}, \beta_{b,1}, \dots, \beta_{b,40}) \leq P'_{\text{sys}} (= 0.0013) \\ & \text{with } \mathbf{M}(\tilde{\mathbf{p}})\ddot{\mathbf{u}}(t, \tilde{\mathbf{p}}) + \mathbf{C}(\tilde{\mathbf{p}})\dot{\mathbf{u}}(t, \tilde{\mathbf{p}}) + \mathbf{K}(\tilde{\mathbf{p}})\mathbf{u}(t, \tilde{\mathbf{p}}) = \mathbf{f}(t, \tilde{\mathbf{p}}) \end{aligned} \quad (22)$$

Topology optimization results and convergence histories are shown in Figure 10 and Figure 11. Final topologies obtained from the optimization problem with two component probabilistic constraints in Eq. (21) and that with the system constraint in Eq. (22) show similar material distributions. However, significantly different topologies from two approaches may be obtained under different optimization and modelling parameters. The optimal volume from the system probabilistic constraint is slightly higher than the one from component probabilistic constraints.

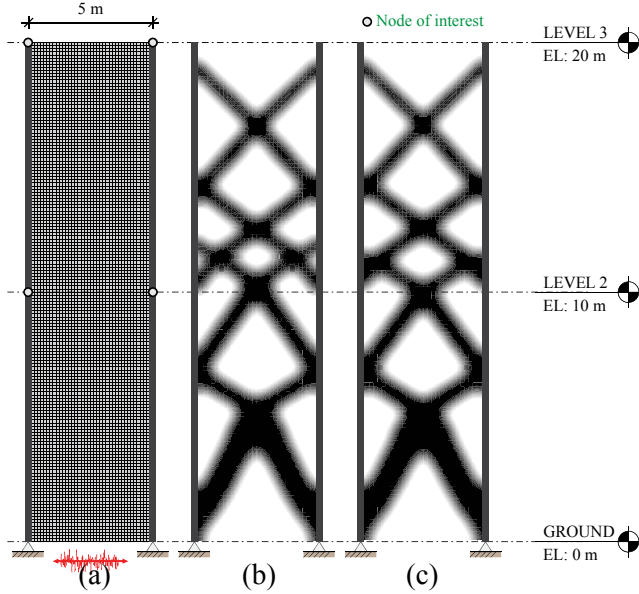


Figure 10: Topology optimization solutions to the multi-story building example ($\beta'_{sys} = 3.0$, $P'_{sys} = 0.13\%$): (a) design domain; (b) system constraint; (c) component constraints.

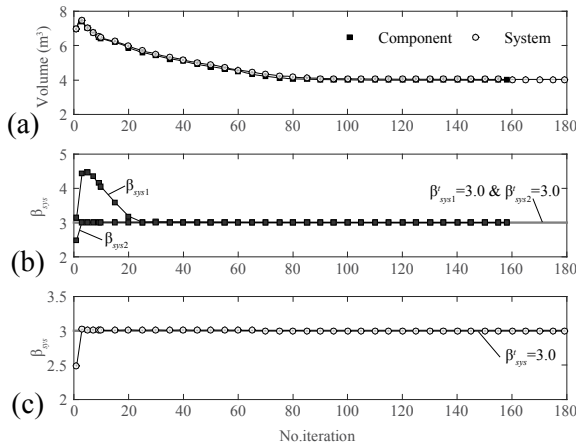


Figure 11: Convergence history. (a) volume; (b) reliability indices of component constraints; (c) reliability index of system constraint.

8. CONCLUSIONS

In this paper, a new topology optimization framework is proposed for structures under stochastic excitations under constraints on first-passage probability. The proposed topology optimization frame work provides an efficient way for structural engineers to obtain optimal design solutions satisfying probabilistic constraints on stochastic response in the conceptual design process of structural systems subject to stochastic excitations.

9. ACKNOWLEDGEMENT

The authors gratefully acknowledge funding provided by the National Science Foundation (NSF) through project CMMI 1234243. We also acknowledge support from the Donald B. and Elizabeth M. Willett endowment at the University of Illinois at Urbana-Champaign. Any opinion, finding, conclusions or recommendations expressed here are those of the authors and do not necessarily reflect the views of the sponsors.

10. REFERENCES

- Bendsøe, M. P., and Sigmund, O. (2003). "Topology optimization – theory, methods and applications." NY, Springer Verlag.
- Bendsøe, M.P., and Sigmund, O. (1999). "Material interpolation schemes in topology optimization." *Archive of Applied Mechanics*, 69(9–10), 635–654.
- Chun, J., and Song, J., and Paulino, G.H. (2013). "System reliability based topology optimization of structures under stochastic excitations." *11th International Conference on Structural Safety & Reliability*, New York, NY.
- Chun, J., and Song, J., and Paulino, G.H. (2015). "Parameter Sensitivity of System Reliability Using Sequential Compounding Method." *Structural safety*, 55, 26–36.
- Chun, J., and Song, J., and Paulino, G.H. (2014). "Topology optimization of structures under stochastic excitation." *Structural and Multidisciplinary Optimization*. Under review.
- Der Kiureghian, A. (2000). "The geometry of random vibrations and solutions by FORM and SORM." *Probabilistic Engineering Mechanics*, 15, 81–90.
- Fujimura, K., and Der Kiureghian, A. (2007). "Tail-equivalent linearization method for nonlinear random vibration." *Probabilistic Engineering Mechanics*, 22(1), 63–76.
- Guest, J.K., and Prevost, J.H., Belytschko, T. (2004). "Achieving minimum length scale in topology optimization using nodal design variables and projection functions." *International Journal for Numerical Methods in Engineering*, 61(2), 238–254.
- Kang, W.H., and Song, J. (2010). "Evaluation of multivariate normal integrals for general systems by sequential compounding." *Structural Safety*, 32(1), 35–41.
- Sigmund, O. (2007). "Morphology-based black and white filters for topology optimization." *Structural and Multidisciplinary Optimization*, 33(4–5), 401–424.
- Song, J., and Der Kiureghian, A. (2006). "Joint first-passage probability and reliability of systems under stochastic excitation." *Journal of Engineering Mechanics*, 132(1), 65–77.
- Song, J., and Kang, W.H. (2009). "System reliability and sensitivity under statistical dependence by matrix-based system reliability method." *Structural Safety*, 31(2), 148–156.
- VanMarcke, E.H. (1975). "On the distribution of the first-passage time for normal stationary random processes." *Journal of Applied Mechanics*, 42, 215–220.